Nanostructured Materials and Functional Coatings
Наноструктурированные материалы и функциональные покрытия

UDC 620.18
https://doi.org/10.17073/1997-308X-2023-2-62-70

Research article
Научная статья

Investigation of the tribological characteristics of Ta–Zr–Si–B–C–N coatings

A. D. Sytchenko ✉, R. A. Vakhrushev, Ph. V. Kiryukhantsev-Korneev

National University of Science and Technology "MISIS"
4 bld.1 Leninskiy Prosp., Moscow 119049, Russia

alina-sytchenko@yandex.ru

Abstract. Ta–Zr–Si–B–C–N coatings were deposited by magnetron sputtering using a $TaSi_2$–Ta_3B_4–(Ta, Zr)B_2 composite target. Ar, as well as Ar + N_2 and Ar + C_2H_4 gas mixtures, were used as the working gas. The structure and composition of the coatings were studied by scanning electron microscopy, glow-discharge optical emission spectroscopy, and *X*-ray diffraction. A Calowear tester was used to measure the thickness and abrasion resistance of the coatings. Erosion resistance tests were carried out using a UZDN-2T (Russia) ultrasonic disperser. Tribological tests in the sliding friction mode were carried out on an HT Tribometer (CSM Instruments, Switzerland) automated friction machine. The wear zone after tribological testing was examined using a Veeco Wyko 1100 (Veeco, USA) optical profiler. The results showed that the Ta–Zr–Si–B coating was characterised by a columnar structure with an *h*-$TaSi_2$ crystallite size of 11 nm. The introduction of nitrogen and carbon into the composition of the coatings led to the suppression of columnar growth and a ~2–4-fold decrease in the size of *h*-$TaSi_2$ crystallites. Carbon-containing coatings demonstrated the best abrasive resistance. The sliding friction tests showed that the Ta–Zr–Si–B coating is characterised by a stable coefficient of friction of 0.3 at a temperature of 25 °C up to the maximum working temperature of 250 °C. The introduction of nitrogen led to an increase in the coefficient of friction up to 0.8–1.0 at a t = 50÷110 °C. The coating with the minimum carbon concentration showed a stable coefficient of friction of ~0.3 up to a maximum temperature of 250 °C. The best result was demonstrated by the sample containing the maximum amount of carbon, with its coefficient of friction remaining at the 0.25 level up to a temperature of 350 °C.

Keywords: magnetron sputtering, coatings, $TaSi_2$, ZrB_2, abrasion and erosion resistance, high-temperature tribology

Acknowledgements: This work was carried out with the financial support of the Russian Science Foundation (project 19-19-00117-П). The authors are grateful to Senior Engineer N.V. Shvyndina (NUST MISIS) for the help in the structural studies.

For citation: Sytchenko A.D., Vakhrushev R.A., Kiryukhantsev-Korneev Ph.V. Investigation of the tribological characteristics of Ta–Zr–Si–B–C–N coatings. *Powder Metallurgy and Functional Coatings*. 2023;17(2):62–70. https://doi.org/10.17073/1997-308X-2023-2-62-70

Исследование триботехнических характеристик покрытий Ta–Zr–Si–B–C–N

А. Д. Сытченко ✉, Р. А. Вахрушев, Ф. В. Кирюханцев-Корнеев

Национальный исследовательский технологический университет «МИСИС»
119049, г. Москва, Ленинский пр-т, 4, стр. 1

alina-sytchenko@yandex.ru

Аннотация. Покрытия Ta–Zr–Si–B–C–N были нанесены методом магнетронного распыления с использованием композиционной мишени $TaSi_2$–Ta_3B_4–(Ta, Zr)B_2. В качестве рабочего газа использовали Ar, а также смеси газов Ar + N_2 и Ar + C_2H_4. Структуру и состав покрытий исследовали методами сканирующей электронной микроскопии,

оптической эмиссионной спектроскопии тлеющего разряда и рентгенофазового анализа. Толщину и стойкость покрытий к абразивному воздействию оценивали по схеме «шарик–шлиф». Испытания на эрозионную стойкость проводили с использованием ультразвукового диспергатора УЗДН-2Т (Россия). Трибологические испытания в режиме трения–скольжения осуществляли на автоматизированной машине трения HT Tribometer («CSM Instruments», Швейцария). Зону износа после трибологических испытаний исследовали с помощью оптического профилометра Wyko 1100 («Veeco», США). Результаты показали, что покрытие Ta–Zr–Si–B характеризуется столбчатой структурой с размером кристаллитов *h*-$TaSi_2$ порядка 11 нм. Введение азота и углерода в состав покрытий привело к подавлению столбчатого роста и снижению размера кристаллитов *h*-$TaSi_2$ в 2–4 раза. Лучшую абразивную и эрозионную стойкость показали углеродсодержащие покрытия. Испытания на трение–скольжение показали, что покрытие Ta–Zr–Si–B характеризуется стабильным коэффициентом трения на уровне 0,3, начиная с 25 °C и до максимальной рабочей температуры 250 °C. Введение азота привело к росту коэффициента трения до значений 0,8–1,0 при $t = 50 \div 110$ °C. Покрытие с минимальной концентрацией углерода показало стабильный коэффициент трения ~0,3 до максимальной температуры 250 °C. Наилучший результат продемонстрировал образец, содержащий наибольшее количество углерода: его коэффициент трения сохранялся на уровне 0,25 до температуры 350 °C.

Ключевые слова: магнетронное напыление, покрытия, $TaSi_2$, ZrB_2, абразивная и эрозионная стойкость, высокотемпературная трибология

Благодарности: Работа выполнена при финансовой поддержке Российского научного фонда (проект 19-19-00117-П).

Авторы признательны ведущему инженеру Н.В. Швындиной (НИТУ МИСИС) за помощь в проведении структурных исследований.

Для цитирования: Сытченко А.Д., Вахрушев Р.А., Кирюханцев-Корнеев Ф.В. Исследование триботехнических характеристик покрытий Ta–Zr–Si–B–C–N. *Известия вузов. Порошковая металлургия и функциональные покрытия*. 2023;17(2):62–70. https://doi.org/10.17073/1997-308X-2023-2-62-70

Introduction

Tantalum disilicide is one of the promising materials in the family of high-temperature ceramics due to its high melting point (2300±100 °C) [1], electrical resistivity (50–70 μΩ·cm) [2], hardness (16 GPa) [3], strength at temperatures above 1000 °C, and good oxidation resistance [4]. $TaSi_2$ coatings are characterised by high thermal stability up to 500 °C and oxidation resistance at 800 °C due to the formation of a Ta_2O_5–SiO_2 oxide layer [5]. Due to their low resistivity (70 μΩ·cm) at $t = 800 \div 900$ °C, $TaSi_2$ coatings are often used in the semiconductor industry [6; 7].

To improve its mechanical and tribological properties and its oxidation resistance, tantalum silicide is doped with various elements such as C, N, B, Hf, and Zr [8–16]. The carbon-doped $TaSi_2$ coating demonstrates good resistance to high-temperature erosion at a thermal flux of 2.4 MW/m^2 [9] and oxidation resistance at $t = 900$ °C for more than 233 h [10]. The authors explain high oxidation resistance as due to the formation of a dense Ta_2O_5–SiO_2 oxide layer. The introduction of nitrogen also improves the mechanical properties and oxidation resistance of $TaSi_2$ coatings.

The study [11] found an extreme dependence of hardness and fracture toughness on the nitrogen content: their maximum values $H = 36$ GPa and $K_{1c} = 3.95$ MPa·m$^{0.5}$, respectively, were reached at a concentration of 35 at. % N. The Ta–Si–N coating is characterised by good oxidation resistance and thermal stability at $t = 700$ °C [12]. In previous studies, the authors studied the structure and properties of Ta–Si–N coatings [13]. The results showed that coatings with an optimal nitrogen concentration had the maximum values of hardness (24 GPa) and elastic recovery (77 %), and also demonstrated high oxidation resistance at $t = 1200$ °C. It is known that introducing nitrogen in Ta–Si–C coatings increases their tribological characteristics at temperatures up to 800 °C due to the formation of the ternary oxide $TaSiO_x$ in the contact area [14].

Research on the effect of the introduction of additives of transition metal borides to the composition of $TaSi_2$-based coatings has been limited to a few studies. Doping Ta–Si–C coatings with zirconium boride [15] increases their adhesive and cohesive strength. The specimens demonstrate good oxidation resistance at $t = 1500$ °C, which may be related to the formation of a protective ZrO_2–SiO_2 oxide layer that prevents oxygen penetration. We have previously investigated the structure and oxidation resistance of Ta–Zr–Si–B–C–N coatings [16] obtained by magnetron sputtering in various gaseous media.

The main objective of this work is to study the tribotechnical characteristics of Ta–Zr–Si–B–C–N coatings exposed to abrasion and erosion impacts and in the sliding friction mode.

Materials and methods

The coatings were deposited by magnetron sputtering in a direct current mode. A sputtered composite target $TaSi_2$–Ta_3B_4–(Ta, Zr)B_2 (composition, at. %: 70.8 Ta, 18.6 Si, 7.4 Zr, 2.9 B) of diameter 120 mm and thickness 6 mm was obtained by hot pressing of crushed products of self-propagating high-temperature synthesis (SHS). Equipment based on the UVN-2M (УВН-2М) pumping system (JSC Kvarts, Russia) with a schematic diagram given in the work [17] was used to deposit the coatings. VOK-100-1 (BOK-100-1) (JSC Polikor, Russia) aluminium oxide plates and disks were used as model substrates for the coatings. Before coating, the substrates were cleaned for 5 min in isopropyl alcohol using a UZDN-2T (УЗДН-2Т) unit (NPP UkrRosPribor, Ukraine) with an operating frequency of 22 kHz and in a vacuum using a gap-type ion source (Ar^+ ions, 2 keV) for 20 min. Ar (99.9995 %) and its mixtures with N_2 (99.999 %) and C_2H_4 (99.95 %) were used as the working gas. The flow rate was controlled using a gas injection system (OOO Eltochpribor, Russia). The values are given in the table.

The coatings were deposited under the following conditions: the distance between the substrate and the target was 80 mm, the residual pressure was 10^{-3} Pa, and the working pressure in the vacuum chamber was 0.1÷0.2 Pa. The magnetron power was kept constant at 1 kW using a Pinnacle+ power supply (Advanced Energy, USA), with a deposition time of 40 min.

The distribution profiles of the elements and the thickness-averaged composition of the coatings were determined using the glow-discharge optical emission spectroscopy (GDOES) method on a Profiler 2 device (Horiba Jobin Yvon, France) [18]. The structure of the coatings was examined by scanning electron microscopy (SEM) using an S-3400 microscope (Hitachi, Japan). *X*-ray diffraction (XRD) was performed on a D2 Phaser diffractometer (Bruker, Germany) using CuK_α-radiation. The *X*-ray photoelectron spectroscopy (XPS) studies were carried out on a PHI 5000 VersaProbe-II (ULVAC-PHI, USA) instrument. The excitation source was monochromatised AlK_α-radiation ($h\nu$ = 1486.6 eV) with a power of 50 W and a diameter of 200 μm.

The thickness and abrasion resistance of the coatings were measured by a Calowear tester (JSC NII Tavtoprom, Russia) according to the ball-specimen set up as described in the methodology [19]. The material was exposed to an abrasive DiaPro suspension with a 1 μm polycrystalline diamond dispersion fed into the gap between a rotating ShKh-15 (ШХ-15) steel ball of diameter 27 mm and the surface of a stationary sample. The ball rotation speed was 13 rpm, and the load was 1.5 N. The volume of the coating material removed was determined using 2D microscopic images.

Abrasion tests were also used to determine the coating thickness using the formula

$$S = \frac{b^2 - a^2}{8R},$$

where b is the wear scar diameter, μm; a is the substrate diameter, μm; R is the ball radius, μm.

The quantity of the coating material removed was calculated using the formula

$$V = \frac{\pi}{64R}\left(b^4 - a^4\right),$$

where b and a are the outer and inner diameters of the crater, respectively, mm.

Erosion tests were carried out using a UZDN-2T (УЗДН-2Т) (NPP UkrRosPribor, Ukraine) ultrasonic disperser. A sample was placed in a container positioned in the working area, after 20 ml of water and 5 g of Si_3N_4 abrasive material were added. The distance from the waveguide to the substrate surface was 1 mm, and the frequency was set at 22 kHz. The experiment lasted 15–60 min. The change in the mass of the coating samples due to erosive impact was estimated using a GR202 (AND, Japan) analytical balance with an accuracy of 0.01 mg.

The coatings were tested for sliding friction on an HT Tribometer (CSM Instruments, Switzerland) auto-

Gas flow rate and chemical composition of the coatings

Расход газа и химический состав покрытий

Sample No.	Gas flow rate, cm^3/min			Composition, at. %					
	Ar	N_2	C_2H_4	Ta	Zr	Si	B	N	C
1	25	–	–	40.0	7.5	28.0	24.5	0	0
2	20	5	–	27.3	7.7	22.3	22.3	20.4	0
3	15	10	–	19.3	5.4	17.1	15.7	42.5	0
4	20	–	5	28.1	10.1	25.7	23.6	0	12.5
5	15	–	10	22.1	8.0	21.1	18.4	0	30.4

mated friction machine using a 6-mm-diameter Al_2O_3 ball as a counter body. The load was 1 N. The change in the coefficient of friction was recorded during heating from a temperature of 25 °C to 500 °C. The contact zones after tribological tests in the abrasive wear and sliding friction modes were examined using a Wyko 1100 (Veeco, USA) optical profiler.

Result and discussion

Composition and microstructure of coatings

The table above shows the elemental composition of the coatings. It can be seen that the concentrations of nitrogen and carbon in the coatings increased with an increase in the N_2 and C_2H_4 gas flow rates, respectively.

Fig. 1, *a* shows the *X*-ray diffraction patterns of the coatings taken in the 2θ = 20÷50° range.

Besides the Al_2O_3 substrate peaks (card JCPDS 88–0107), the *X*-ray diffraction pattern of coating *1* showed peaks corresponding to the hexagonal *h*-$TaSi_2$ phase (JCPDS 89-2941). Note that the differences in the intensity of the peaks from the Al_2O_3 substrate may be associated with a change in the composition and amorphisation of the coatings as a result of the introduction of nitrogen or carbon. The size of the *h*-$TaSi_2$ crystallites, determined by the Scherrer equation, was 11 nm. The introduction of N_2 and C_2H_4 into the gaseous medium resulted in the formation of coatings with a highly dispersed or amorphous structure. For nitrogen- and carbon-containing coatings, the peak maxima positions in the 2θ = 25÷45° range were close to the positions of the most intense peaks of the TaN (JCPDS 89–5198) and TaC (JCPDS 89–3831) FCC phases.

The crystallite size of the *h*-$TaSi_2$ phase for reactive coatings *2–5* was estimated from minimally overlapping lines. For coatings *2* and *3* deposited at an N_2 flow rate of 5 and 10 cm^3/min, the sizes were 6.0 and 4.5 nm, while for carbon-containing coatings *4* and *5*, they were similar at 3.5 and 3.0 nm, respectively. The decrease in the size of *h*-$TaSi_2$ crystallites and the amorphisation of coatings upon transition to reaction media are associated with the formation of new TaN and TaC phases, which, apparently, interrupt the growth of *h*-$TaSi_2$ crystallites.

According to the SEM images, base coating *1* had a columnar structure (see Fig. 1, *b*). It is important to note that this phenomenon adversely affects the mechanical properties and oxidation resistance of coatings [20; 21]. All reactive coatings showed an identical structure. The introduction of N_2 and C_2H_4 into the gas medium led to the suppression of columnar growth and the formation of highly dispersed crystallites.

The Calowear tester measurements showed coatings *1* and *2* as having a similar thickness of 7.2 and

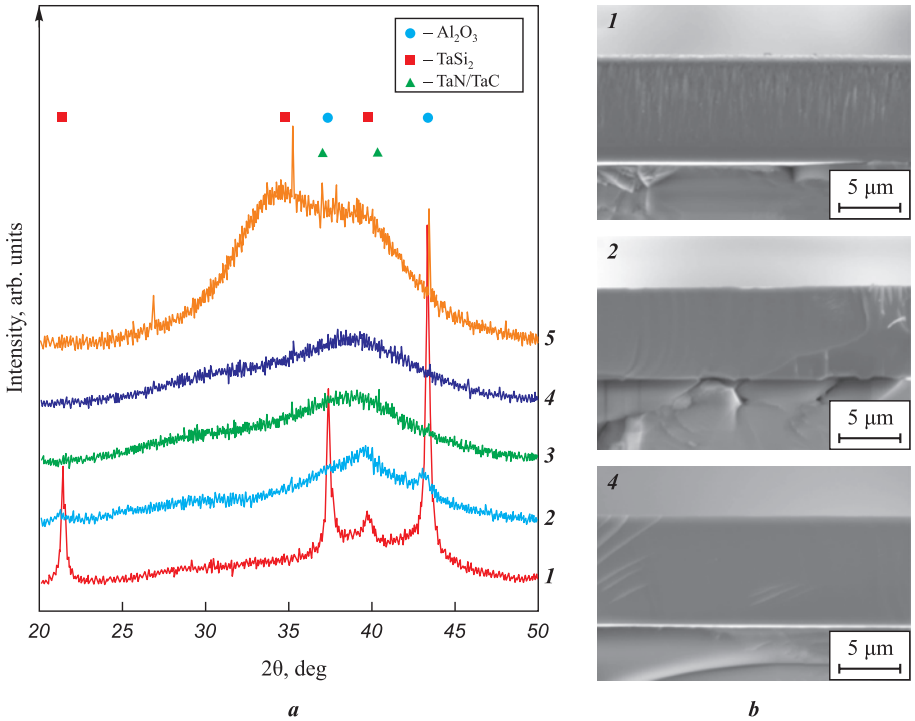

Fig. 1. *X*-ray diffraction patterns of the coatings ***1–5*** (***a***) and cross-section SEM images of the coatings ***1***, ***2*** and ***4*** (***b***)

Рис. 1. Рентгенограммы покрытий ***1–5*** (***a***) и СЭМ-изображения поперечного излома покрытий ***1***, ***2*** и ***4*** (***b***)

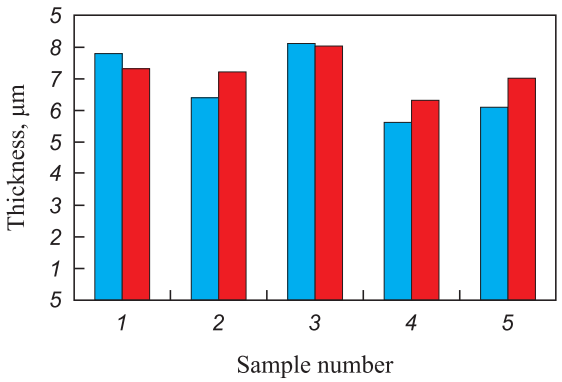

Fig. 2. Comparison of the thicknesses of coatings ***1–5*** obtained by the Calowear tester (■) and from the cross-section SEM images of the coatings (■)

Рис. 2. Сравнение значений толщины покрытий ***1–5***, полученных методами «шарик–шлиф» (■) и по СЭМ-изображениям поперечных изломов (■)

7.0 μm, respectively (Fig. 2). An increase in nitrogen concentration led to its growth by 25 %. In [11], a similar result was obtained related to an increase in the thickness of coatings with an increase in the N_2 gas flow rate. Increasing the C_2H_4 flow rate to 5 and 10 cm^3/min led to a decrease in thickness by 18 and 10 %, respectively. The Calowear tester measurements were compared with the thickness values determined from the fracture cross-section SEM images of the coatings (Fig. 2). The results obtained were similar. This method can therefore be used for the rapid assessment of coating thicknesses.

Erosion resistance

The trial tests allowed determining the optimal mode in which the wear of the coatings (abrasive material – Si_3N_4, its mass – 5 g, liquid volume – 20 ml) was observed. The graph in Fig. 3 shows the dependence of the change in mass on the time of exposure to abrasive particles.

Coating *1* obtained in the Ar medium was observed to have the minimum mass loss Δm = –0.2 mg throughout the experiment. For coating *2*, the value of Δm increased to 0.2 mg over a 0–30 min interval, which is probably due to the adhesion of wear products and abrasive particles on the sample surface. The subsequent decrease in mass by 3.8 mg over a 30–60 min interval is due to coating wear (Fig. 3, *b*). Coating *3* had the value Δm = –0.3 mg over a 60 min interval, which corresponds to the data obtained for the non-reactive coating. Unstable behaviour was observed for the carbon-containing sample *4*: the Δm value increased by 1.0 mg over a 0–15 min interval, after which at 15–30 min of exposure it dropped to the initial values. Over a 30–60 min interval, Δm = 0.8 mg. Coating *5* with the maximum carbon concentration had Δm = 1.5 mg over a 0–15 min interval, after which the sample mass gradually decreased and by the 60th minute of the test approached the initial value ($\Delta m \approx$ –0.1 mg).

Visual inspection of the samples revealed no signs of wear on the coating surface *1* (Fig. 3, *b*). The coatings obtained in nitrogen had a clear circular wear boundary with noticeable areas of the substrate, whereas the samples obtained in ethylene had less pronounced wear marks and no areas corresponding to the substrate.

The samples obtained in Ar and Ar + C_2H_4 media therefore showed the best erosion resistance. The high erosion resistance of carbon-containing coatings can be explained by the increased hardness of the TaC carbide phase compared to the TaN and $TaSi_2$ phases [22; 23].

Abrasion resistance

The results of the abrasive tests showed that scratches from the impact of abrasive particles were observed on the surfaces of all samples. Fig. 4 shows the depths (H) and thickness (h) of wear craters under abrasive action for coatings *1–5*.

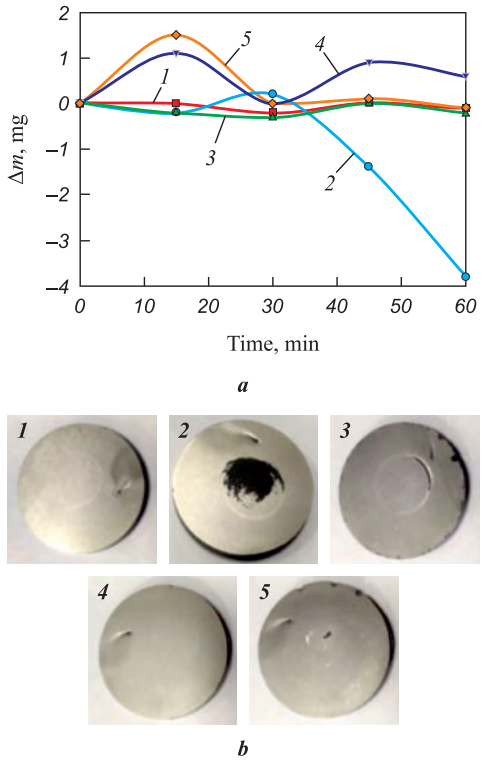

Fig. 3. Dependence of the change in mass on the time of exposure to abrasive particles (***a***) and photographs of samples after 60 min of exposure (***b***)
1–5 – numbers of coating samples

Рис. 3. График зависимости изменения массы от времени воздействия абразивных частиц (***a***) и фотографии образцов после 60 мин воздействия (***b***)
1–5 – номера образцов покрытий

Fig. 5 shows the dependence of the volume of material removed (V) on the abrasive exposure time (1- and 3-min) for the studied samples. Coatings *1*, *3–5* showed similar values of $H = 4 \div 5$ μm and $V = 5 \div 6 \cdot 10^{-4}$ mm^3, respectively, differing within the error margin. The nitrogen-containing coating *2* has maximum values of $H = 5$ μm and $V = 11 \cdot 10^{-4}$ mm^3. With an increase in the exposure time to 3 min, coatings *1–3* had crater depths in the range of 6–7 μm, and the volume of the removed material was $24 \cdot 10^{-4}$ mm^3. Note that the crater depths did not exceed the thickness of the samples *1–3*. After a 3-minute exposure, coating *4* had an H value of 7 μm at a thickness of 6 μm, which is indicative of wear. In this case, the sample was characterised by a lower value of $V = 18 \cdot 10^{-4}$ mm^3 compared to coatings *1–3*, which may be due to the influence of the solid Al_2O_3 substrate. Coating *5* with the lowest carbon concentration showed the minimum results ($H = 5.5$ μm and $V = 15 \cdot 10^{-4}$ mm^3).

Summing up the data obtained, it can be concluded that the coating deposited at the maximum concentration of ethylene has better abrasive resistance, which may be due to the positive role of carbon in the friction process [24].

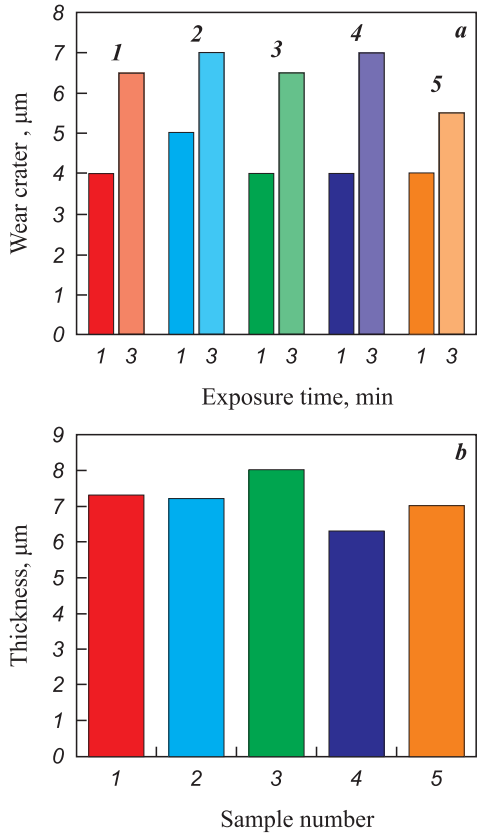

Fig. 4. Depth (***a***) and thickness (***б***) of wear craters under abrasive action over 1- and 3-min intervals for coatings ***1–5***

Рис. 4. Глубина кратеров износа (***а***) и толщина (***б***) при абразивном воздействии в течение 1 и 3 мин для покрытий ***1–5***

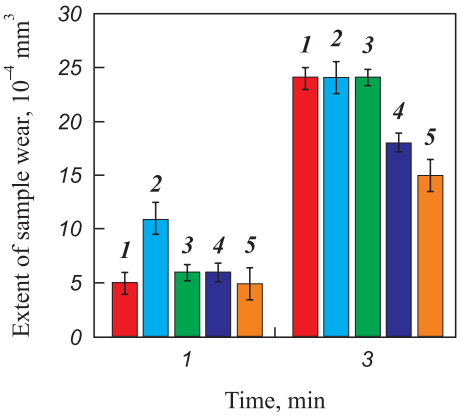

Fig. 5. Extent of sample wear during abrasive exposure over 1- and 3-min intervals for coatings ***1–5***

Рис. 5. Объем износа образца при абразивном воздействии в течение 1 и 3 мин для покрытий ***1–5***

Tribological tests in the sliding friction mode

Fig. 6 shows the results of tribological testing of coatings in the sliding friction mode during heating from a temperature of 25 °C to 500 °C.

Coating 1 showed a stable coefficient of friction of μ ~0.3 up to $t = 225$ °C. Above this temperature, the value of μ increased to >0.8, which is indicative of coating wear. Sample *2* had an unstable coefficient of friction over the entire temperature range. Over the 25–110 °C range, there was a rapid increase of the μ value from 0.2 to 0.82, which may be associated with the formation of friction wear products. A further decrease in μ to 0.3 is due to the removal of wear products from the tribocontact zone. After a stable interval from 150 to 210 °C, the value of μ gradually increased until it exceeded the 0.8 value at $t = 400$ °C.

Coating 3 with the maximum nitrogen content showed a sharp increase in μ to ~1 at $t = 25 \div 50$ °C. The effect of an increase in the coefficient of friction to values close to 1 may be associated with the exit to the substrate and the friction of the counter body material (Al_2O_3) over the Al_2O_3 substrate, accompanied by adhesive interaction. A similar process was described in detail in [25] in the example of the emergence of a steel-to-steel tribocontact. Sample *4* with the minimum carbon content showed a stable value of μ ~0.3 up to a temperature of 250 °C. In the range $t = 250 \div 350$ °C, an increase in μ to 0.9–1.0 was observed. Coating *5* with the maximum carbon concentration demonstrated the best result, with its coefficient of friction having a stable value of 0.25 up to a temperature of 350 °C. According to the literature data, the Ta–Si–C–N coating is characterised by a high coefficient of friction of 0.6 at $t = 300 \div 400$ °C [26]. Note

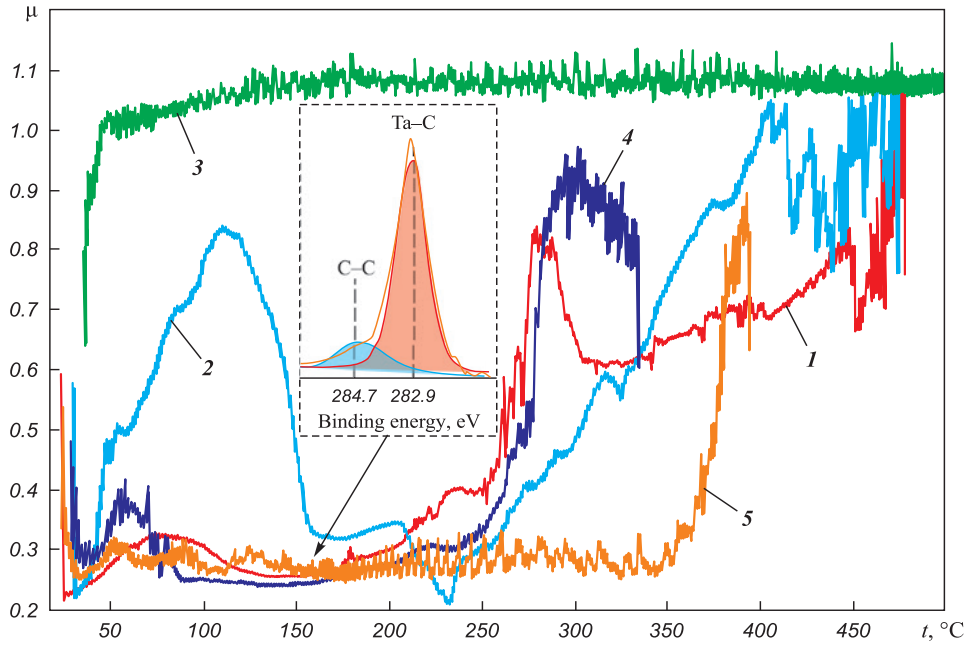

Fig. 6. Dependence of the coefficient of friction on temperature
The inset shows the C1*s* spectrum for coating ***5*** obtained by *X*-ray photoelectron spectroscopy

Рис. 6. Зависимость коэффициента трения от температуры
На вставке представлен спектр C1*s* для покрытия ***5***, полученный методом рентгеновской фотоэлектронной спектроскопии

that the value of μ = 0.25 for sample *5* is half the value obtained earlier for the Ta–Si–C–N coating.

Thus, the coating obtained at a 10 cm^3/min flow rate of C_2H_4 has the minimum coefficient of friction μ = 0.25 and the maximum operating temperature of 350 °C. To determine the reason for the decrease in the coefficient of friction with increasing carbon concentration, coating *5* was studied by *X*-ray photoelectron spectroscopy (see Fig. 6). In the C1*s* spectrum, peaks were observed at a binding energy of 282.9 and 284.4 eV, indicating the presence of Ta–C and C–C bonds, respectively [27; 28]. The reduced coefficient of friction may be associated with the positive role of free carbon, which in some cases can be released during supersaturation of the crystalline carbide phase and acts as a solid lubricant during friction [29]. The influence of the *Me*C carbide phase with a lower coefficient of friction compared to the *Me*N nitride phase also cannot be ruled out [30].

Conclusion

In this work, Ta–Zr–Si–B–C–N system coatings were obtained by magnetron sputtering method using a $TaSi_2$–Ta_3B_4–(Ta, Zr)B_2 target. Ar, as well as Ar + N_2 and Ar + C_2H_4 mixtures, were used as the working gas. The nonreactive Ta–Zr–Si–B coating was characterised by a columnar structure with a crystallite size of the *h*-$TaSi_2$ hexagonal phase of about 11 nm. When N_2 and C_2H_4 were introduced into the working medium, a change in the columnar structure to an equiaxed one with an *h*-$TaSi_2$ grain size of about 3–6 nm was observed. The thickness of the coatings was between 6.0 and 8.1 μm.

Abrasive tests showed that, when exposed for 1–3 min, the sample obtained at the maximum concentration of ethylene has the best abrasive resistance. This effect is associated with the positive role of carbon, which functions as a solid lubricant during friction.

Erosion tests showed that the base sample has the minimum mass change of –0.2 mg. The introduction of nitrogen did not affect the erosion resistance, and the weight loss values for samples *2* and *3* were –0.2 and –0.3 mg, respectively. The introduction of C_2H_4 into the working medium promoted the growth of Δ*m* to 1.1–1.5 mg. No wear was observed on the surface of carbon-containing samples, which indicates their better erosion resistance.

The sliding friction tests showed that coating *1* has a stable coefficient of friction μ = 0.3 up to the maximum working temperature of 225 °C. The introduction of nitrogen led to an increase in the μ values of the coatings up to 0.8–1.0 and a decrease of the maximum operating temperature to 50–110 °C. The coating with the minimum carbon concentration was characterised by a coefficient of friction of ~0.3 up to 250 °C, which is close to the values for the non-reactive coating. Sample *5* containing the maximum content of carbon showed the best result, with its coefficient of friction remaining at the 0.25 level up to a temperature of 350 °C.

References / Список литературы

1. Samsonov G.V., Dvorina L.A., Rud B.M. Silicides. Vol. 1. Moscow: Metallurgiya, 1979. 272 p. (In Russ.).

   Самсонов Г.В., Дворина Л.А., Рудь Б.М. Силициды. Т. 1. М.: Металлургия, 1979. 272 с.
2. Schultes G., Schmitt M., Goettel D., Freitag-Weber O. Strain sensitivity of TiB_2, $TiSi_2$, $TaSi_2$ and WSi_2 thin films as possible candidates for high temperature strain gauges. *Sensors and Actuators A: Physical*. 2006;126(2):287–291. http://doi.org/10.1016/j.sna.2005.05.023
3. Sciti D., Silvestroni L., Celotti G., Melandri C., Guicciardi S. Sintering and mechanical properties of ZrB_2–$TaSi_2$ and HfB_2–$TaSi_2$ ceramic composites. *Journal of the American Ceramic Society*. 2008;91(10):3285–3291. http://doi.org/10.1111/j.1551-2916.2008.02593.x
4. Shon I.J., Ko I.Y., Chae S.M., Na K.I. Rapid consolidation of nanostructured $TaSi_2$ from mechanochemically synthesized powder by high frequency induction heated sintering. *Ceramics International*. 2011;37(2):679–682. https://doi.org/10.1016/j.ceramint.2010.09.054
5. Niu Y., Huang L., Zhai C., Zeng Y., Zheng X., Ding C. Microstructure and thermal stability of $TaSi_2$ coating fabricated by vacuum plasma spray. *Surface and Coatings Technology*. 2015;279:1–8. https://doi.org/10.1016/j.surfcoat.2015.08.025
6. Blanquet E., Vahlas C., Madar R., Palleau J., Torres J., Bernard C. A thermodynamic and experimental approach to $TaSi_2$ chemical vapour deposition. *Thin Solid Films*. 1989;177(1): 189–206. http://doi.org/10.1016/0040-6090(89)90567-1
7. Mansour A.N. Effect of temperature on microstructure and electrical properties of $TaSi_2$ thin films grown on Si substrates. *Vacuum*. 2011;85(6):667–671. https://doi.org/10.1016/j.vacuum.2010.10.003
8. Zhang M., Ren X., Chu H., Lv J., Li W., Wang W., Yang Q., Feng P. Oxidation inhibition behaviors of the HfB_2–SiC–$TaSi_2$ coating for carbon structural materials at 1700 °C. *Corrosion Science*. 2020;177:108982. https://doi.org/10.1016/j.corsci.2020.108982
9. Liu F., Li H., Gu S., Yao X., Fu Q. Ablation behavior and thermal protection performance of $TaSi_2$ coating for SiC coated carbon/carbon composites. *Ceramics International*. 2019;45(3):3256–3262. https://doi.org/10.1016/j.ceramint.2018.10.230
10. Shi X., Zeng X., Li H., Fu Q., Zou J. $TaSi_2$ oxidation protective coating for SiC coated carbon/carbon composites. *Rare Metal Materials and Engineering*. 2011;40(3):403–406. https://doi.org/10.1016/S1875-5372(11)60024-6
11. Monclús M.A., Yang L., López-Cabañas I., Castillo-Rodríguez M., Zaman A., Wang J., Meletis E.I., González-Arrabal R., Llorca J., Molina-Aldareguía J.M. High temperature mechanical properties and microstructure of hard TaSiN coatings. *Materials Science and Engineering: A*. 2020;797:139976. https://doi.org/10.1016/j.msea.2020.139976
12. Mešić B., Schroeder H. Properties of TaSiN thin films deposited by reactive radio frequency magnetron sputtering. *Thin Solid Films*. 2012;520(13):4497–4500. https://doi.org/10.1016/j.tsf.2012.02.068
13. Sytchenko A.D., Levashov E.A., Kiryukhantsev-Korneev P.V. Structure and properties of Ta–Si–N coatings obtained by pulsed magnetron sputtering. *Russian Journal of Non-Ferrous Metals*. 2021;62(5):611–617. https://doi.org/10.3103/S1067821221050151

   Сытченко А.Д., Левашов Е.А., Кирюханцев-Корнеев Ф.В. Структура и свойства покрытий Ta–Si–N, полученных методом импульсного магнетронного распыления. *Известия вузов. Порошковая металлургия и функциональные покрытия*. 2021;15(2):60–67. https://doi.org/10.17073/1997-308X-2021-2-60-67
14. Bondarev A.V., Vorotilo S.A., Shchetinin I.V., Levashov E.A., Shtansky D.V. Fabrication of Ta–Si–C targets and their utilization for deposition of low friction wear resistant nanocomposite Si–Ta–C–(N) coatings intended for wide temperature range tribological applications. *Surface and Coatings Technology*. 2019;359:342–353. https://doi.org/10.1016/j.surfcoat.2018.12.030
15. Ren Y., Qian Y., Xu J., Jiang Y., Zuo J., Li M. Oxidation and cracking/spallation resistance of ZrB_2–SiC–$TaSi_2$–Si coating on siliconized graphite at 1500 °C in air. *Ceramics International*. 2020;46(5):6254–6261. https://doi.org/10.1016/j.ceramint.2019.11.095
16. Kiryukhantsev-Korneev Ph.V., Sytchenko A.D., Vorotilo S.A., Klechkovskaya V.V., Lopatin V.Y., Levashov E.A. Structure, oxidation resistance, mechanical, and tribological properties of N- and C-doped Ta–Zr–Si–B hard protective coatings obtained by reactive D.C. magnetron sputtering of TaZrSiB ceramic cathode. *Coatings*. 2020;10(10):946. https://doi.org/10.3390/coatings10100946
17. Kiryukhantsev-Korneev Ph.V., Sytchenko A.D., Sviridova T.A., Sidorenko D.A., Andreev N.V., Klechkovskaya V.V., Polčak J., Levashov E.A. Effects of doping with Zr and Hf on the structure and properties of Mo–Si–B coatings obtained by magnetron sputtering of composite targets. *Surface and Coatings Technology*. 2022;442:128141. https://doi.org/10.1016/j.surfcoat.2022.128141
18. Kiryukhantsev-Korneev F.V. Possibilities of glow discharge optical emission spectroscopy in the investigation of coatings. *Russian Journal of Non-Ferrous Metals*. 2014;55(5): 494–504. http://doi.org/10.3103/S1067821214050137

   Кирюханцев-Корнеев Ф.В. Возможности метода оптической эмиссионной спектроскопии тлеющего разряда GDOES при исследовании покрытий. *Известия вузов. Порошковая металлургия и функциональные покрытия*. 2013;(2):60–70. https://doi.org/10.17073/1997-308X-2013-2-60-70
19. Kiryukhantsev-Korneev P.V., Phiri J., Gladkov V.I., Ratnikov S.N., Yakovlev M.G., Levashov E.A. Erosion and abrasion resistance, mechanical properties, and structure of the TiN, Ti–Cr–Al–N and Cr–Al–Ti–N coatings deposited by CFUBMS. *Protection of Metals and Physical Chemistry of Surfaces*. 2019;55(5):913–923. https://doi.org/10.1134/S2070205119050125
20. Mirzaei S., Alishahi M., Souček P., Ženíšek J., Holec D., Koutná N., Buršíková V., Stupavská M., Zábranský L., Burmeister F., Blug B., Czigány Zs., Balázsi K., Mikšová R., Vašina P. The effect of chemical composition on the structure, chemistry and mechanical properties of magnetron sputtered W–B–C coatings: *Modeling and Experiments. Surface and Coatings Technology*. 2020;383: 125274. https://doi.org/10.1016/j.surfcoat.2019.125274
21. Musil J. Hard nanocomposite coatings: Thermal stability, oxidation resistance and toughness. *Surface and Coatings*

Technology. 2012;207:50–65. https://doi.org/10.1016/j.surfcoat.2012.05.073

22. Hu J., Li H., Li J., Huang J., Kong J., Zhu H., Xiong D. Structure, mechanical and tribological properties of TaC_x composite films with different graphite powers. *Journal of Alloys and Compounds*. 2020;832:153769. https://doi.org/10.1016/j.jallcom.2020.153769
23. Nah J.W., Hwang S.K., Lee C.M. Development of a complex heat resistant hard coating based on (Ta, Si)N by reactive sputtering. *Materials Chemistry and Physics*. 2000;62(2): 115–121.https://doi.org/10.1016/S0254-0584(99)00142-X
24. Martínez-Martínez D., López-Cartes C., Justo A., Fernández A., Sánchez-López J.C. Self-lubricating Ti–C–N nanocomposite coatings prepared by double magnetron sputtering. *Solid State Sciences*. 2009;11(3):660–670. https://doi.org/10.1016/j.solidstatesciences.2008.10.017
25. Kiryukhantsev-Korneev P.V., Pierson J.F., Bychkova M.Y., Manakova O.S., Levashov E.A., Shtansky D.V. Comparative study of sliding, scratching, and impact-loading behavior of hard CrB_2 and Cr–B–N films. *Tribology Letters*. 2016;63(3):44. https://doi.org/10.1007/s11249-016-0729-0
26. Bondarev A.V., Antonyuk M.N., Kiryukhantsev-Korneev Ph.V., Polcar T., Shtansky D.V. Insight into high temperature performance of magnetron sputtered Si–Ta–C–(N) coatings with an ion-implanted interlayer. *Applied Surface Science*. 2021;541:148526. https://doi.org/10.1016/j.apsusc.2020.148526
27. *XPS Database*. http://www.lasurface.com/database/elementxps.php
28. Vargas M., Castillo H.A., Restrepo-Parra E., De La Cruz W. Stoichiometry behavior of TaN, TaCN and TaC thin films produced by magnetron sputtering. *Applied Surface Science*. 2013;279:7–12. https://doi.org/10.1016/j.apsusc.2013.03.028
29. Sánchez-López J.C., Martínez-Martínez D., López-Cartes C., Fernández A. Tribological behaviour of titanium carbide/amorphous carbon nanocomposite coatings: From macro to the micro-scale. *Surface and Coatings Technology*. 2008;202(16):4011–4018. https://doi.org/10.1016/j.surfcoat.2008.02.012
30. González-Hernández A., Morales-Cepeda A.B., Caicedo J.C., Amaya C., Olive-Méndez S.F. Structure, functional groups analysis and tribo-mechanical behavior of carbide and nitride coatings deposited on AISI 1060 substrates by RF-magnetron sputtering. *Journal of Materials Research and Technology*. 2022;18:5432–5443. https://doi.org/10.1016/j.jmrt.2022.04.075

Information about the Authors

Alina D. Sytchenko – Junior Research Scientist of the "*In situ* Diagnostics of Structural Transformations" Laboratory of Scientific-Educational Center of Self-Propagating High-Temperature Synthesis (SHS), MISIS–ISMAN, National University of Science and Technology (NUST) "MISIS"
ORCID: 0000-0002-8668-5877
E-mail: alina-sytchenko@yandex.ru

Roman A. Vakhrushev – MSc, Laboratory Assistant Researcher of the "*In situ* Diagnostics of Structural Transformations" Laboratory of Scientific-Educational Center of SHS, MISIS–ISMAN
E-mail: romavahaa@gmail.com

Philipp V. Kiryukhantsev-Korneev – Cand. Sci. (Eng.), Associate Professor, Department of Powder Metallurgy and Functional Coatings of NUST "MISIS"; Head of the "*In situ* Diagnostics of Structural Transformations" Laboratory of Scientific-Educational Center of SHS, MISIS–ISMAN
ORCID: 0000-0003-1635-4746
E-mail: kiruhancev-korneev@yandex.ru

Сведения об авторах

Алина Дмитриевна Сытченко – мл. науч. сотрудник лаборатории «*In situ* диагностика структурных превращений» научно-учебного центра (НУЦ) СВС, МИСИС–ИСМАН, Национальный исследовательский технологический университет (НИТУ) «МИСИС»
ORCID: 0000-0002-8668-5877
E-mail: alina-sytchenko@yandex.ru

Роман Алексеевич Вахрушев – магистрант, лаборант-исследователь лаборатории «*In situ* диагностика структурных превращений», НУЦ СВС, МИСИС-ИСМАН
E-mail: romavahaa@gmail.com

Филипп Владимирович Кирюханцев-Корнеев – к.т.н, доцент кафедры порошковой металлургии и функциональных покрытий НИТУ МИСИС; зав. лабораторией «*In situ* диагностика структурных превращений», НУЦ СВС, МИСИС–ИСМАН
ORCID: 0000-0003-1635-4746
E-mail: kiruhancev-korneev@yandex.ru

Contribution of the Authors

A. D. Sytchenko – conducting the calculations, writing the text, testing the samples; analysis of the research results, writing the text, formulation of the conclusions.
R. A. Vakhrushev – testing the samples, writing the text.

Ph. V. Kiryukhantsev-Korneev – formation of the main concept, goal and objectives of the study; scientific guidance, correction of the text and conclusions.

Вклад авторов

А. Д. Сытченко – проведение расчетов, испытаний образцов, анализ результатов исследований, подготовка текста, формулировка выводов.
Р. А. Вахрушев – проведение испытаний образцов, подготовка текста статьи.
Ф. В. Кирюханцев-Корнеев – формирование основной концепции, постановка цели и задачи исследования, научное руководство, корректировка текста, корректировка выводов.

Received 28.06.2022
Revised 01.11.2022
Accepted 08.11.2022

Статья поступила 28.06.2022 г.
Доработана 01.11.2022 г.
Принята к публикации 08.11.2022 г.